ELSEVIER
Cold Regions Science and Technology 30 (1999) 135–144
cold regions science and technology
www.elsevier.com/locate/coldregions

Simulation of above treeline snowdrift formation using a numerical snow-transport model

Ethan M. Greene *, Glen E. Liston, Roger A. Pielke Sr.

Department of Atmospheric Science, Colorado State University, Fort Collins, CO, 80523 USA

Received 24 November 1998; accepted 9 March 1999

Abstract

A physically based, numerical snow-transport model (SnowTran-3D) is used to successfully simulate the above treeline snowdrift evolution around Montgomery Pass in the Northern Colorado Rocky Mountains. The model accounts for key snow-transport components including: saltation, suspension, deposition, erosion, and sublimation. The snow-transport model requires static inputs of vegetation type and topography, and temporally evolving spatial distributions of air temperature, humidity, precipitation, wind speed, and wind direction. A simple wind-flow model, driven by data from a ridge-top meteorological station, is used to simulate the flow field over the topographic drift catchment. The snow-transport model outputs include the spatial and temporal evolution of snow depth resulting from variations in precipitation, saltation and suspension transport, and sublimation. The model is forced using SNOTEL and meteorological data from the 1997–1998 winter, and the resulting model outputs are compared with observed snowdrift distributions.

Keywords: Numerical snow-transport model; Wind-flow model; Snowdrift evolution

1. Introduction

The redistribution of snow by wind is a major contributing factor to the spatial and temporal distribution of seasonal snowcovers. In alpine environments it is a dominant force behind the distribution of snow, and also plays a key role in determining the amount of snowcover returned to the atmosphere by sublimation (Schmidt, 1972, 1991). Hence, the physical processes associated with blowing and drifting snow are of importance to a wide scope of disciplines. The ability to accurately simulate or predict snow redistribution by wind can improve spring runoff predictions in terms of both magnitude and spatial variability, especially in areas where snow has been blown into a neighboring drainage catchment. Redistribution of snow also affects the spatial distribution of early-season soil moisture which can directly influence agriculture production (Olienyk et al., 1979), and alpine germination and growth (Evans et al., 1989; Walker et al., 1993). Reliable calculations of snow-mass redistribution by wind into

* Corresponding author.

0165-232X/99/$ - see front matter
PII: S0165-232X(99)00008-7

avalanche-path starting zones would allow more accurate avalanche stability predictions, assisting avalanche forecasters in their efforts to safeguard highways and ski areas, and provide stability information for backcountry areas (Perla, 1970; LaChapelle, 1980; Buser et al., 1985; Schmidt and Hartman, 1986; Ferguson et al., 1990; McClung and Schaerer, 1993; Birkeland, 1997). Improvements in our understanding and ability to simulate the erosion and deposition of seasonal snow are expected to assist advancements in hydrology, agriculture, and avalanche forecasting and safety.

There have been many previous efforts to model snowdrift formation. Many of these efforts have approached this process as a two-dimensional problem (Berg and Caine, 1975; Tabler, 1975; Berg, 1986; Liston et al., 1993; Sundsbø, 1997). These studies examined snow transport over a barrier, creating snow-distribution profiles on the windward and lee sides of the barrier. The Prairie Blowing Snow Model (Pomeroy et al., 1993) included important processes such as sublimation in a blowing snow model capable of simulating equilibrium transport under steady-state conditions.

Fewer studies have attempted to model the three-dimensional distribution of snow deposited by wind. Using a model which computed the air flow and predicted snowdrift rates, Uematsu (1993) simulated snowdrifts over a level surface, and Uematsu et al. (1991) simulated wind-flow patterns and snow distributions around a small building and small hill. Pomeroy et al. (1997) modified the Prairie Blowing Snow Model for use in the Arctic. The model was driven by monthly mean climatological data and produced an end-of-winter snow distribution. A rule- and cell-based model of snow transport and distribution has also been applied to a three-dimensional snow-distribution problem in Scotland (Purves et al., 1998). Liston and Sturm (1998) developed and used a model to reproduce the three-dimensional, wind-modified snow distribution in Arctic Alaska. This model performed well for a site which included complex terrain devoid of trees.

In the current study, the Liston and Sturm model (SnowTran-3D) is applied to a Colorado alpine site. The central feature of the study area is an above treeline, north/south running ridge-line. Daily-averaged atmospheric fields are used as input to drive the model, and the modeled snowdrift distribution is compared to the observed snow distribution.

2. Site description

Montgomery Pass is situated in an alpine portion of the northern Colorado Rocky Mountains. North of Rocky Mountain National Park and Colorado Highway 14, the pass lies in the Colorado State Forest section of the Medicine Bow Mountains. At an elevation of 3333 m, Montgomery Pass is above treeline and part of a north/south running ridge-line (Fig. 1).

The simulation domain is centered on the ridge-line containing Montgomery Pass. The pass lies near

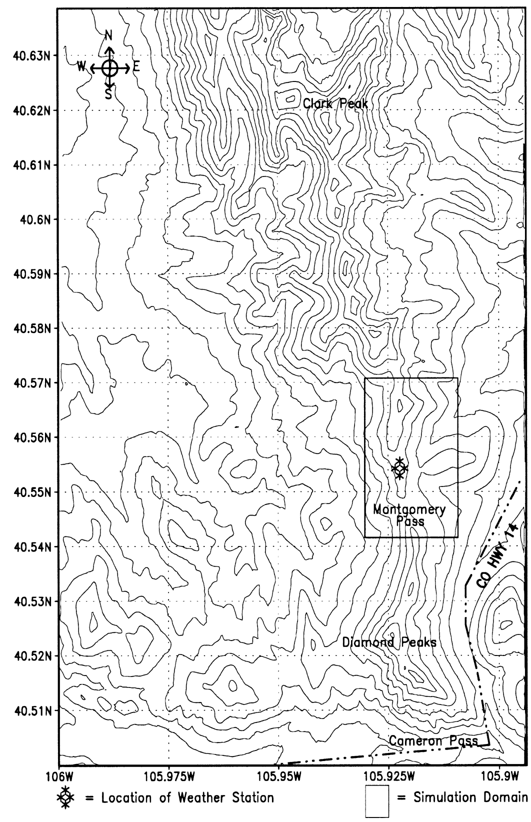

Fig. 1. USGS 7.5-min quadrangle for Clark Peak Colorado. Montgomery Pass lies on the main north/south running ridge-line. The Cache La Poudre river drainage lies to the east of the pass, and North Park lies to the west.

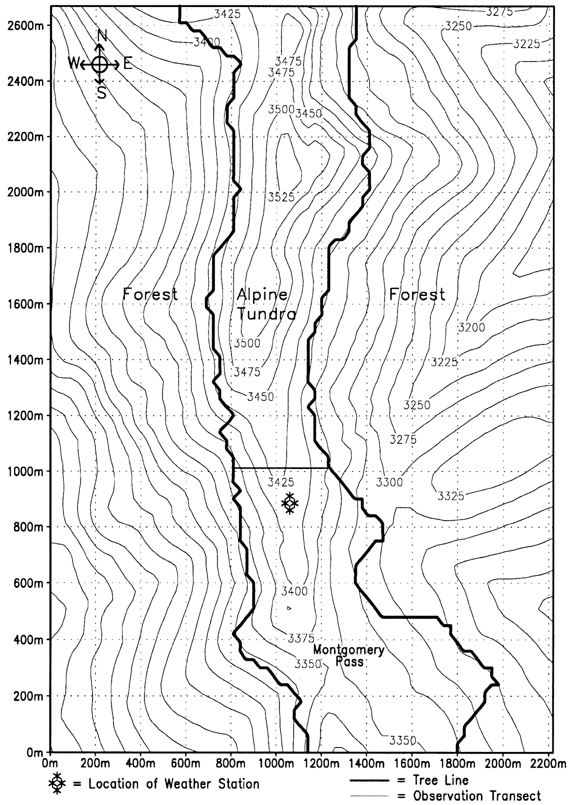

Fig. 2. Topography and vegetation for the model simulation domain. Contour interval is 25 m. Treeline marks the division between evergreen forest and alpine tundra. Also shown is the location of the remote weather station and the observation transect.

the southern boundary of the domain (Fig. 2). Elevations within the simulation domain range between 3175 and 3521 m above sea level. The domain is 2.7 km along the north/south axis, 2.25 km along the east west axis, and includes dense forest cover on both sides of the ridge-line.

3. Field procedures

In mid-December 1997, a 3 m tower and instrumentation array were installed on the ridge-line 800 m north of Montgomery Pass (Fig. 2). The array contained instruments capable of recording air temperature, relative humidity, wind direction, and wind speed. Thirty-minute averages of these observations were saved on a Campbell CR-10 data logger. The weather station was in place from December 1997 until April 1998. Precipitation measurements were obtained from the Natural Resources Conservation Service SNOTEL site at Joe Wright Creek. The Joe Wright Creek site lies 4 km to the southeast at 3066 m above sea level.

On February 18, 1998 the snow depth was observed along an east/west-running transect. The transect extended from the east treeline to the west treeline and crossed the ridge crest near the weather station site. Using a set of probes, snow-depth measurements were taken at 5-m intervals along this transect (Fig. 2). These data were used to verify the SnowTran-3D simulations.

4. Model description

SnowTran-3D was developed to simulate blowing snow processes in complex terrain (Liston and Sturm, 1998). The snow-transport model is fully three-dimensional, in that it is implemented in two horizontal dimensions (x and y), and evolves the snow and snow-water-equivalent depth (the z dimension) over a topographically variable domain. The model considers only transport variations resulting from accelerating and decelerating flow (i.e., convergent and

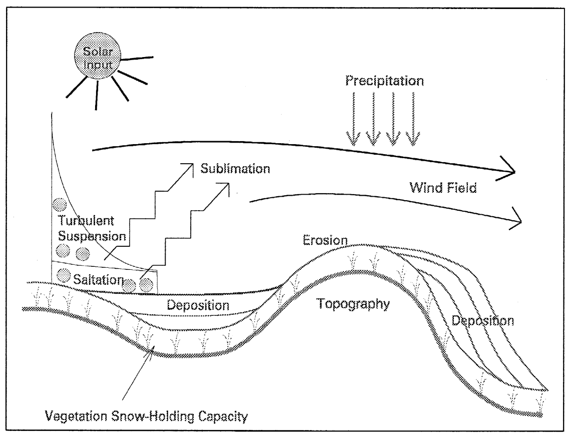

Fig. 3. Key features of the snow-transport model applied to topographically variable terrain (from Liston and Sturm, 1998).

divergent wind fields); non-equilibrium transport due to temporal wind-speed accelerations and decelerations (e.g., transport variations due to turbulent wind fluctuations) are not accounted for. The topography within the domain can vary from flat, to gently rolling, to highly varying, such as regions where flow separation might occur over sharp ridges, gullies, or valleys.

Fig. 3 illustrates the key input parameters (solar radiation, precipitation, wind speed and direction, air temperature, humidity, topography, vegetation snow-holding capacity), the key processes (saltation, turbulent-suspension, sublimation), and the key outputs (spatial distribution of snow erosion and deposition) from the model. The six primary components of the snow-transport model are: (1) the computation of the wind-flow forcing field; (2) the wind-shear stress on the surface; (3) the transport of snow by saltation; (4) the transport of snow by turbulent-suspension; (5) the sublimation of saltating and suspended snow; and (6) the accumulation and erosion of snow at the snow surface, a lower boundary that is allowed to move with time.

The foundation of this snow-transport model is a mass-balance equation which describes the temporal variation of snow depth at a point. Deposition and erosion, which lead to changes in snow depth at this point are the result of (1) changes in horizontal mass-transport rates of saltation, Q_s (kg/(m s)), (2) changes in horizontal mass-transport rates of turbulent-suspended snow, Q_t (kg/(m s)), (3) sublimation of transported snow particles, Q_v (kg m^{-2} s^{-1}), and

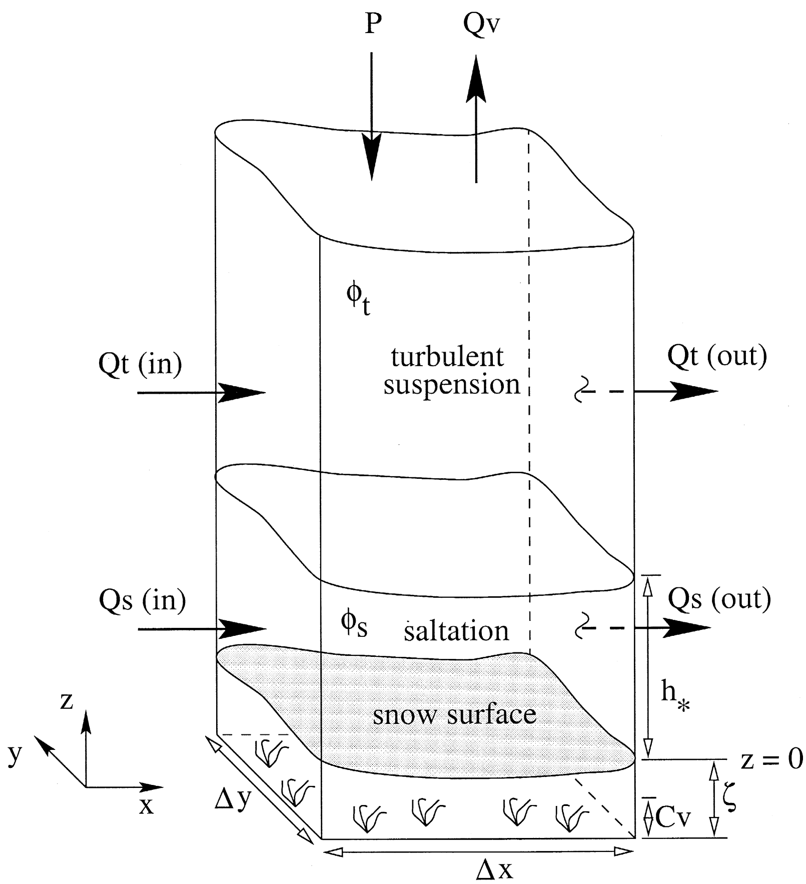

Fig. 4. Schematic of the SnowTran-3D snow-transport model mass-balance computation (from Liston and Sturm, 1998).

(4) the water-equivalent precipitation rate, P (m s^{-1}). Combined, the time rate of change of snow depth, ζ (m), is

$$\frac{d\zeta}{dt} = \frac{1}{\rho_s} \times \left(\rho_w P - \left(\frac{dQ_s}{dx} + \frac{dQ_t}{dx} + \frac{dQ_s}{dy} + \frac{dQ_t}{dy} \right) + Q_v \right) \quad (1)$$

where t (s) is time; x (m) and y (m) are the horizontal coordinates in the west–east and south–north directions, respectively; and ρ_s and ρ_w (kg/m) are the snow and water density, respectively. Fig. 4 provides a schematic of this mass-balance accounting. Eq. (1) is solved for each individual grid cell within a domain, and is coupled to the neighboring cells through the spatial derivatives (d/dx, d/dy). Complete details of the formulation of each term in Eq. (1) can be found in Liston and Sturm (1998).

To drive the snow-transport model, a reference-level wind-flow field over the domain of interest is required at each model time-step. This wind field is generated by taking observed wind speeds and directions, and interpolating them to the model grid. The wind distribution is modified to account for topographic influences, by multiplying with an empirically based weighting factor, W,

$$W = 1.0 + \gamma_s \Omega_s + \gamma_c \Omega_c \quad (2)$$

where Ω_s and Ω_c are the topographic slope and curvature, respectively, in the direction of the wind, and γ_s and γ_c are positive constants which weight the relative influence of Ω_s and Ω_c on modifying the wind speed. The slope and curvature are computed such that lee and concave slopes produce Ω_s and Ω_c less than zero, and that windward and convex slopes produce Ω_s and Ω_c greater than zero. Thus, lee and concave slopes produce reduced wind speeds, and windward and convex slopes produce increased wind speeds.

5. Methodology

For this study the model uses a 30-m grid over the previously described domain (Fig. 2). Temporal integrations were computed daily for 56 days. This time period spanned from the installation of the weather station (December 24, 1997), until the snow depth transect was observed (February 18, 1998).

Many studies have shown that precipitation amounts vary with location and elevation in mountainous terrain (Hjermstad, 1970; Johnson and Hanson, 1994; Baopu, 1995; Snook and Pielke, 1995; Obleitner and Mayr, 1996). The simulations for this study were initially run with the observed precipitation from Joe Wright Creek. These simulations produced a snowdrift distribution similar to that observed. However, the modeled drift mass was less than the observed drift mass. In order to compensate for the difference in elevation between the study site and the Joe Wright Creek SNOTEL site, the precipitation was increased until the model-simulated drift mass was within 1% of the observed. This compensation for elevation differences increased the period precipitation by 2%. The combination of the atmospheric data collected by the instrumentation array, and the adjusted precipitation data from the SNOTEL site were used to drive SnowTran-3D during these simulations.

Since the initial snowdrift distribution was unknown, the model was initialized with the October thru December precipitation from the Joe Wright Creek SNOTEL site. The initial precipitation was subject to the same elevation compensation as the daily precipitation. This initial snowcover was as-

Table 1
User-defined constants used in model simulations

C_v		vegetation holding snow-capacity (m)
	5.0	evergreen trees
	0.003	alpine tundra
z_{0_veg}		vegetation roughness length (m)
	0.80	evergreen trees (Pielke, 1984)
	0.10	alpine tundra
f	500.0	equilibrium fetch distance (m) (Pomeroy et al., 1993)
u_{*t}	0.25	threshold wind shear velocity (m/s) (Schmidt, 1986)
z_{0_snow}	0.005	snow roughness length (m)
Y_c	400	topographic curvature weighting factor
Y_s	10	topographic slope weighting factor
μ	3.0	scaling constant for non-equilibrium saltation transport
ρ_s	350.0	snow density (kg/m^3)
σ_c	0.5	cloud cover faction

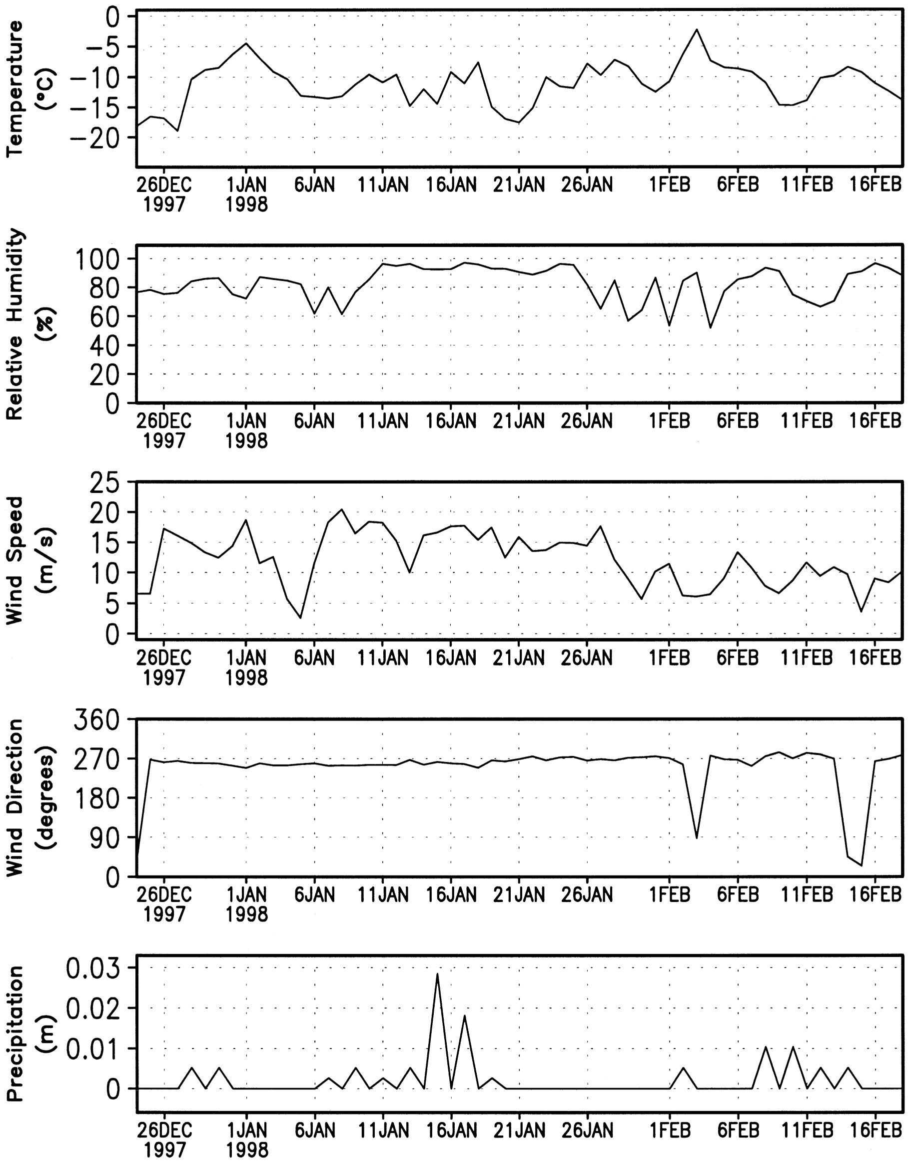

Fig. 5. December 24, 1997 thru February 18, 1998 daily average atmospheric forcing data of air temperature, relative humidity, wind speed, wind direction, and snow-water-equivalent precipitation used in model simulations.

signed a density of 350 kg/m^3; the average density observed from snowpits in the study area. To run SnowTran-3D, several other parameters must be defined, such as the threshold shear stress, the surface roughness length, and the vegetation snow-holding capacity. Values for the parameters used in the simulation are summarized in Table 1. In addition, the atmospheric forcing data used to drive the model (air temperature, relative humidity, wind speed, wind direction, and precipitation) are given in Fig. 5.

6. Results

Due to persistent westerly winds with velocities greater than 5 m/s (Fig. 5), the majority of the snow on the west side of the terrain barrier was eroded away and transported to the east side of the barrier. The model was able to adequately simulate the snow drift distribution across the terrain barrier (Fig. 6). In the treed areas the winter snowpack remained unaltered, while in the above-treeline areas the snowpack was eroded down to the surface holding capacity (Table 1). The general snow-distribution profile, and the relationships between treed windward and lee slopes are illustrated in Fig. 7, where the simulated snow depth has been enhanced by a factor of 3 in order to make it easier to see the snow distribution. On the east side of the terrain barrier the model deposited the snow in a well-defined row of drifts which runs parallel to, and between the ridge-crest and the eastern treeline (Fig. 8).

As part of the snow-transport scheme, the model computes the mass of snow removed from the domain due to sublimation of the blowing snow. Dividing this value by the total precipitation input (both initialized and daily precipitation) yields the mass fraction of the snow removed by sublimation. Over the ridge-crest, between 9% and 15% of the snow was returned to the atmosphere by sublimation (Fig. 9). Isolated points along the terrain barrier sublimated up to 30% of the period precipitation. These numbers are consistent with the findings of Pomeroy and Gray (1995) and Liston and Sturm (1998) for

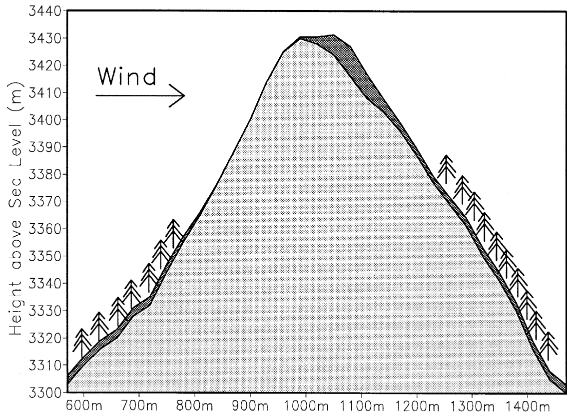

Fig. 7. Snowdrift profile along observed transect. The snow depth is enhanced by a factor of 3.

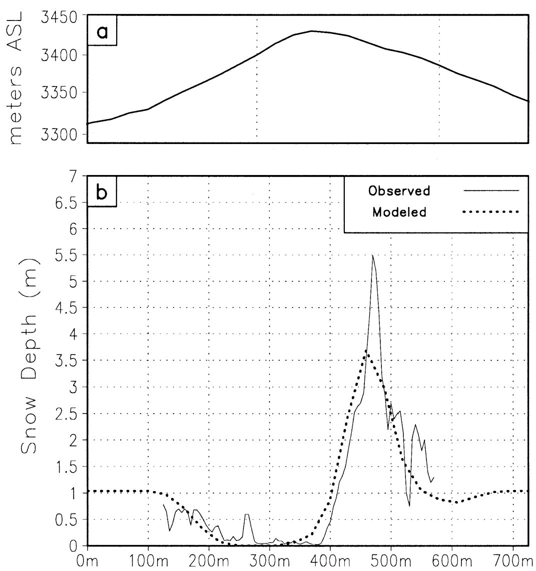

Fig. 6. (a) Cross section of model topography at the location of the observed transect. The ordinate indicates meters above sea level. (b) Cross section of modeled and observed snow depths (m) for February 18, 1998.

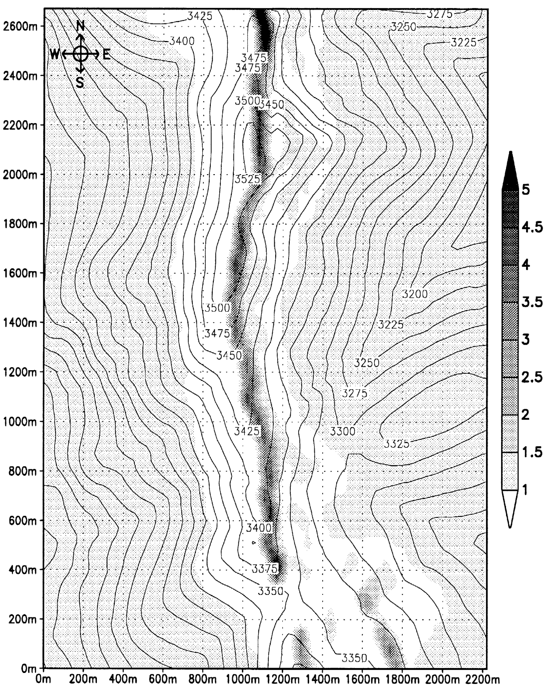

Fig. 8. Model-simulated spatial distribution of snow depth (m) for February 18, 1998.

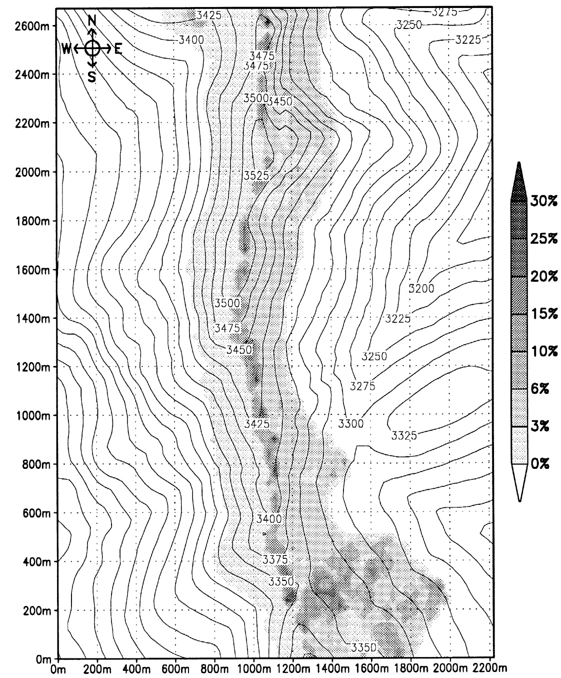

Fig. 9. Percent of year-to-date (February 18, 1998) snow-water-equivalent removed by sublimation of airborne snow.

regions of the Canadian Prairies and Arctic North America.

7. Discussion

The model simulation produced a snowdrift profile which compares well with the observed profile. Fig. 6 shows that the simulated drift has a similar slope and width to the observed drift. The model was also able to simulate the rapid decrease in snow depth at the transition from treeline to alpine tundra on the west side of the terrain barrier (Figs. 6 and 8). The maximum depth of the observed drift is nearly 2 m greater than the simulated drift. We consider this result acceptable due to the difference in resolution between the observations and the model grid (model $\Delta x = 30$ m, observations $\Delta x = 5$ m). Although the observations show a peak depth of 5.5 m, it is a sharp peak occurring over a distance of 10 m. At the current resolution, the model is unable to resolve features of this scale.

It is difficult to obtain a quantitative figure for the amount of sublimation which should occur in this type of environment. The physical process is nonlinear and cannot be measured remotely. The model calculates the amount of sublimation using the atmospheric fields provided. However, we have no way of determining the error in these calculations. If our precipitation estimates do not adequately compensate for the elevation differences, it may be due, in part, to insufficient sublimation values calculated by the model.

The least substantiated method used during this study was the precipitation adjustment for elevation differences. Although it is widely accepted that in mountainous regions precipitation varies with location and elevation, a method for adjusting precipitation data which is both reliable and universal has not yet been established. In a high alpine area, such as Montgomery Pass, it is difficult to directly measure snowfall accurately due to relatively high winds.

8. Conclusions

The weather at the study site was characterized by persistent winds with velocities at or above the threshold speed for transport (Schmidt, 1980; McClung and Schaerer, 1993; Li and Pomeroy, 1997). Due to the combined effects of synoptic weather patterns and topography the dominant wind direction was from the west. This resulted in the majority of the above-treeline snowpack being eroded from the west side of the ridgeline, and being transported and deposited on the east side. The model simulated the physical processes associated with the wind-transport of snow, building a drift on the east side of the terrain barrier whose location, width and slope compared well with observations. Given the difference in scales between the model grid and observation interval, the height of the drift also compared well with the observations. An improved precipitation data set, obtained from a position closer to the research site, would have allowed further scrutiny of the model's sublimation calculations.

Blowing and drifting snow, and the snow distributions which these processes create, have relevance to many disciplines. The ability to accurately predict this phenomena can enhance work being done to improve safety and heighten economic goals. Examples of this include, more accurate spring runoff estimates, the capture of snow to improve spring soil moisture conditions for agricultural production, and more accurate avalanche forecasts leading to shorter periods where transportation arteries are closed for control work. In addition, the implementation of a wind and blowing snow model, with the ability to be run in real time, could substantially assist avalanche prediction and control efforts in both the public and private sectors. This study is put forth as an initial demonstration that the tools and techniques required to simulate snow redistribution by wind are now becoming available.

Acknowledgements

The work described here was sponsored by NOAA grant NA67RJ015. The authors would like to thank Dr. William Malm of the National Park Service Air Resources Division, Air Resource Specialists, and Dr. Tom McKee of The Colorado Climate Center for the use of remote meteorological instrumentation. Special thanks is also extended to Dr. Kelly Elder, Roger Tree, John Kleist, Walt Nalor, and Terry Flint for their individual advice and assistance.

References

Baopu, F., 1995. The effects of orography on precipitation. Boundary-Layer Meteorol. 75, 189–205.

Berg, N.H., 1986. A deterministic model for snowdrift accumulation. Proceedings of the International Snow Science Workshop, Tahoe, CA, pp. 29–36.

Berg, N., Caine, N., 1975. Prediction of natural snowdrift accumulation in alpine areas. Final Report to Rocky Mountain Forest and Range Expt. Station (USFS 19-388-CA), Dept. of Geography, University of Colorado, Boulder, 69 pp.

Birkeland, K.W., 1997. Spatial and temporal variations in snow stability and snowpack conditions throughout the Bridger Mountains, Montana. PhD dissertation, Arizona State University, pp. 161, 168, 174.

Buser, O., Fohn, P., Good, W., Gubler, H., Salm, B., 1985. Different methods for the assessment of avalanche danger. Cold Reg. Sci. Technol. 10, 199–218.

Evans, B.M., Walker, D.A., Benson, C.S., Nordstrand, E.A., Petersen, G.W., 1989. Spatial interrelations between terrain, snow distributions and vegetation patterns at an Arctic foothills site in Alaska. Holarctic Ecol. 12, 270–278.

Ferguson, S.A., Moore, M.B., Marriott, R.T., Speers-Hayes, P., 1990. Avalanche weather forecasting at the northwest Avalanche Center, Seattle, Washington, USA. J. Glaciol. 36, 57–66.

Hjermstad, L.M., 1970. Influence of meteorological parameters on the distribution of precipitation across central Colorado mountains. Colorado State University Scientific Paper No. 163. Colorado State University, Fort Collins, CO.

Johnson, G.L., Hanson, C.L., 1994. Topographic and atmospheric influences on precipitation variability over a mountainous watershed. J. Appl. Meteorol. 34, 68–87.

LaChapelle, E.R., 1980. The fundamental processes in conventional avalanche forecasting. J. Glaciol. 26, 75–84.

Li, L., Pomeroy, J.W., 1997. Estimates of threshold wind speeds for snow transport using meteorological data. J. Appl. Meteorol. 36, 205–213.

Liston, G.E., Sturm, M., 1998. A snow-transport model for complex terrain. J. Glaciol. 44, 498–516.

Liston, G.E., Brown, R.L., Dent, J., 1993. A two-dimensional computational model of turbulent atmospheric surface flows with drifting snow. Ann. Glaciol. 18, 281–286.

McClung, D., Schaerer, P., 1993. The Avalanche Handbook. The Mountaineers, Seattle, pp. 27–30.

Obleitner, F., Mayr, G.J., 1996. On the mesoscale structure of the intra-Alpine precipitation distribution during a typical winter snowfall event. Meteorol. Z. 5, 110–120.

Olienyk, J.P., Snyder, J.R., Skold, M.D., Willis, W.O., 1979. The economic benefits and costs of managing windblown snow in the Northern Plains of the US. Proceedings of the Fifth International Conference on Wind Engineering, July 1979, Fort Collins, CO, pp. 37–46.

Perla, R.I., 1970. On contributory factors in avalanche hazard evaluation. Can. Geotech. J. 7, 414–419.

Pielke, R.A., 1984. Mesoscale Meteorological Modeling. Academic Press, p. 143.

Pomeroy, J.W., Gray, D.M., 1995. Snowcover accumulation, relocation and management. National Hydrology Research Institute Science Report No. 7, Hydrological Sciences Division, NHRI Division of Hydrology, University of Saskatchewan, Saskatoon, p. 144.

Pomeroy, J.W., Gray, D.M., Landine, P.G., 1993. The Prairie Blowing Snow Model: characteristics, validation, operation. J. Hydrol. 144, 165–192.

Pomeroy, J.W., Marsh, P., Gray, D.M., 1997. Application of a distributed blowing snow model to the Arctic. Hydrol. Processes 11, 1451–1464.

Purves, R.S., Barton, J.S., Mackaness, W.A., Sugden, D.E., 1998. The development of a rule-based spatial model of wind transport and deposition of snow. Ann. Glaciol. 26, 196–202.

Schmidt, R.A., 1972. Sublimation of wind-transported snow-A model. Res. Pap. RM-90 Rocky Mtn. For. and Range Expt. Sta. For. Serv. U.S. Dept. of Agric., Fort Collins, CO.

Schmidt, R.A., 1980. Threshold wind-speeds and elastic impact in snow transport. J. Glaciol. 26, 453–467.

Schmidt, R.A., 1986. Transport rate of drifting snow and the mean wind speed profile. Boundary-Layer Meteorol. 34, 213–241.

Schmidt, R.A., 1991. Sublimation of snow intercepted by an artificial conifer. Agric. Forest Meteorol. 54, 1–27.

Schmidt, R.A., Hartman, H., 1986. Storage and redistribution of snow upwind of an avalanche catchment. Proceedings of the International Snow Science Workshop, Tahoe, CA, pp. 37–40.

Snook, J.S., Pielke, R.A., 1995. Diagnosing a Colorado heavy snow event with a nonhydrostatic mesoscale numerical model structured for operational use. Weather and Forecasting 10, 261–285.

Sundsbø, P.A., 1997. Numerical modelling and simulation of snow drift. Ph.D Dissertation, The Norwegian University of Science and Technology, Trondheim, Norway. Narvik Institute of Technology, Department of Building Science, Narvik, Norway, p. 112.

Tabler, R.D., 1975. Predicting profiles of snowdrifts in topographic catchments. Proceedings of the 43rd Annual Western Snow Conference, San Diego, CA, pp. 87–97.

Uematsu, T., 1993. Numerical study on snow transport and drift formation. Ann. Glaciol. 18, 135–141.

Uematsu, T., Nakata, T., Takeuchi, K., Arisawa, Y., Kaneda, Y., 1991. Three-dimensional numerical simulation of snowdrift. Cold Reg. Sci. Technol. 20, 65–73.

Walker, D.A., Halfpenny, J.C., Walker, M.D., Wessman, C.A., 1993. Long-term studies of snow–vegetation interactions. BioScience 43, 287–301.